ZEBRAFISH
Volume 14, Number 4, 2017

DOI: 10.1089/zeb.2016.1412

A Fully Automated High-Throughput Zebrafish Behavioral Ototoxicity Assay

Douglas W. Todd,[1] Rohit C. Philip,[1] Maki Niihori,[2,3] Ryan A. Ringle,[2] Kelsey R. Coyle,[2] Sobia F. Zehri,[2] Leanne Zabala,[2,4] Jordan A. Mudery,[2,4] Ross H. Francis,[2,4] Jeffrey J. Rodriguez, PhD,[1] and Abraham Jacob[2,3,5,6]

Abstract

Zebrafish animal models lend themselves to behavioral assays that can facilitate rapid screening of ototoxic, otoprotective, and otoregenerative drugs. Structurally similar to human inner ear hair cells, the mechanosensory hair cells on their lateral line allow the zebrafish to sense water flow and orient head-to-current in a behavior called rheotaxis. This rheotaxis behavior deteriorates in a dose-dependent manner with increased exposure to the ototoxin cisplatin, thereby establishing itself as an excellent biomarker for anatomic damage to lateral line hair cells. Building on work by our group and others, we have built a new, fully automated high-throughput behavioral assay system that uses automated image analysis techniques to quantify rheotaxis behavior. This novel system consists of a custom-designed swimming apparatus and imaging system consisting of network-controlled Raspberry Pi microcomputers capturing infrared video. Automated analysis techniques detect individual zebrafish, compute their orientation, and quantify the rheotaxis behavior of a zebrafish test population, producing a powerful, high-throughput behavioral assay. Using our fully automated biological assay to test a standardized ototoxic dose of cisplatin against varying doses of compounds that protect or regenerate hair cells may facilitate rapid translation of candidate drugs into preclinical mammalian models of hearing loss.

Keywords: zebrafish, ototoxicity, rheotaxis, behavioral assay, hearing and hearing loss, drug discovery and development

Introduction

Hearing loss is the most prevalent sensory deficit in humans. About 1 per 1000 children are born deaf, and 3–4 per 1000 develop significant hearing loss during childhood.[1] For children, 30%–50% of hearing loss is hereditary, another 19%–25% is acquired, and in 25%–48% of cases, the cause is unknown.[1] The incidence of hearing loss increases with age, with several population-based studies of patients older than 65 years estimating its prevalence at 42%–47%.[2–4] Tinnitus and hearing loss due to noise exposure top the list of war-related health costs, and according to the DOD Hearing Center of Excellence website (http://hearing.health.mil), over 1.5 million veterans are affected. Veterans receiving service-connected disability for tinnitus and hearing loss increased 13%–18% per year since 2000, costing the Department of Veterans Affairs $2.6 billion in 2014.

In 2008, the World Health Organization estimated that disabling hearing loss affected 360 million people worldwide; and for 2015, their projected estimates were over 700 million affected.[5] Hearing problems cause communication difficulties, social isolation, depression, and decreased quality of life, while recent studies have linked auditory deprivation to progressive cognitive decline and early onset dementia.[6] Therefore, successful research identifying drugs that preserve or improve hearing would have a profound impact on global public health.

In addition to congenital, genetic, syndromic, and age- and noise-induced hearing loss, ototoxicity is a common cause of inner ear damage. Chemotherapeutic agents are major contributors; in fact, ototoxic compounds such as cisplatin are known to damage cochlear hair cells that transduce sound-related mechanical energy into electrical energy for subsequent activation of the auditory nerve.[7–9] Regardless of upstream insult, cochlear hair cells are thought to undergo degeneration

[1]Department of Electrical and Computer Engineering, The University of Arizona, Tucson, Arizona.
[2]Department of Otolaryngology, The University of Arizona, Tucson, Arizona.
[3]The University of Arizona Cancer Center, Tucson, Arizona.
[4]College of Medicine, The University of Arizona, Tucson, Arizona.
[5]BIO5 Institute, The University of Arizona, Tucson, Arizona.
[6]Ear & Hearing, Center for Neurosciences, Tucson, Arizona.

through final common pathways that involve oxidative stress and free radical-mediated damage.[10–12] Unlike age and noise, however, ototoxicity is much easier to model experimentally in high-throughput biologically based systems,[13] especially for testing therapeutics. Therefore, drug discovery using ototoxicity models to screen compounds may secure results that can then be applied more broadly to treat other causes of hearing loss such as noise or aging.

Over the past decade, zebrafish lateral line ototoxicity assays have emerged as powerful biological model systems for drug development targeting hearing loss. Most efforts have focused on anatomic assays of zebrafish lateral line hair cells, inducing ototoxic damage and utilizing hair cell counts or damage scores to assay rescue by candidate drugs.[14] Ton and Parng,[15] Harris *et al.*,[16] Owens *et al.*,[17] and so on, have developed assays for investigating hair cell death and regeneration using zebrafish animal models, which were reviewed by Coffin *et al.*[18] Ou *et al.* used the zebrafish lateral line to screen for drugs that prevent and cause hearing loss.[19] Buck *et al.* used a histological assay to show that hair cell damage occurs in a concentration-dependent manner.[20] Ou *et al.* established that cisplatin causes repeatable and predictable damage to zebrafish lateral line hair cells.[21] Behavioral assays that study zebrafish swimming behavior and determine whether anatomically preserved/rescued hair cells are truly functional, serve as a complement to anatomic assays.

Adult fish exhibit a swimming behavior known as rheotaxis, an innate tendency to swim against the flow of an oncoming current (positive rheotaxis). In the basic form of rheotaxis, the fish detect currents directly by flow over the body surface and head upstream by swimming against the current.[22] Zebrafish also use this detection of the direction of current to position themselves in an appropriate position for catching food floating downstream.[23] In addition, juvenile salmon were also shown to have used rheotactic response (negative rheotaxis: swimming with the flow of water) to move downstream with the current.[24] The influence of the lateral line on rheotaxis behavior has been studied in blind cavefish with differing conclusions on the necessity of the lateral line to mediate rheotaxis.[25,26] Nevertheless, lateral line ablation reduces rheotaxis and flow-related behavior in zebrafish, but does not abolish it.[20,23,27]

Zebrafish, including larval zebrafish, also exhibit rheotaxis under flow conditions. This rheotactic behavior has been widely studied in the literature,[13,27–31] as a response to visual stimuli, vibrations, and so on. Experimentally, as populations of healthy fish are observed when no water is flowing, fish orientation should be random with 1/6 of the population swimming upstream within 30° of the current. Once flow is introduced and the population of fish is then observed over time, a greater fraction of healthy fish should be oriented upstream. Suli and colleagues[23] first evaluated the potential link between rheotactic behavior and lateral line hair cell damage using the ototoxin neomycin. Their work, using a single chamber fish apparatus, still images, and software analysis, determined that there was a tight correlation, establishing reduced rheotaxis behavior as a potential biomarker for functional damage to lateral line hair cells. They also determined that input from other sensory systems, in addition to vision, and the lateral line must feed into the rheotaxis circuitry, indicating that changes in rheotaxis are quite subtle.

Niihori *et al.*[13] have shown that rheotaxis index (RI), the percentage of zebrafish swimming upstream within 30° of the flow of water current, also deteriorates in response to cisplatin exposure. The incremental advance beyond prior work by Suli[23] was their ability to test six distinct populations of fish using a more robust, multichamber fish swimming apparatus, proof-of-principle for use of rheotaxis measures as a platform for high-throughput drug discovery. Although this behavioral system obtained results faster than anatomic assays of hair cell integrity, manual acquisition of still images and subsequent calculation of fish swimming angles by hand were still required.[13]

In this article, we describe dramatic advances in technology that have considerably improved this behavioral assay[13] as a drug discovery platform. A truly high-throughput swimming apparatus has been built, which automatically computes RIs for large numbers of zebrafish test populations in a fraction of the time it takes trained experts to manually quantify rheotactic index. This scalable system includes a custom-designed imaging system that acquires a high-definition video of zebrafish test populations swimming in darkness. In addition, the increased number of custom-designed swimming lanes facilitates rapid analysis of a large number of ototoxicity experiments performed in parallel, thereby increasing the capability of the behavioral assay to comprehensively screen hundreds or even thousands of potentially otoprotective compounds. Furthermore, we have developed customized image analysis software that detects and segments individual zebrafish larvae, determines their orientations against the flow of water current, and automatically computes RI. These robust algorithms now output RI data tables through an intranet user interface. Automatic RI computation also eliminates subjective variation inherently present in manual analysis of data by different operators, resulting in more consistent results. In this study, we describe the swimming apparatus itself, imaging system, image analysis techniques, and experimental results to validate that our next-generation behavioral assay produces RI values consistent with manual analysis, but with much greater throughput.

Materials and Methods

Zebrafish care and breeding

Zebrafish embryos were obtained from parings of AB wild-type adult fish and maintained in an E2 embryo medium (15.0 mM NaCl, 0.5 mM KCl, 1.0 mM $MgSO_4$, 0.15 mM KH_2PO_4, 0.05 mM Na_2HPO_4, 1.0 mM $CaCl_2$, and 0.7 mM $NaHCO_3$) at a density of 50 embryos per 100-mm Petri dish. All zebrafish were housed in a Zebrafish Aquatic Housing System (Aquaneering, Inc., San Diego, CA) located at the University of Arizona's animal care facility under the following environmental conditions: light–dark cycle, 14–10 h, with water temperature controlled at 28.5°C ± 0.5°C. Five days postfertilized (dpf) or older larvae were fed by rotifer polyculture or GEMMA micro 75 powder food (SKRETTING a Nutreco Company, ME). The University of Arizona's Institutional Animal Care and Use Committee approved all animal procedures.

Anatomic assay

After the drug exposure, zebrafish larvae were fluorescently labeled in an embryo medium containing 6 μM YO-PRO-1 (Y3603; Invitrogen) for 20 min, to quantify the anatomic

damage sustained by zebrafish lateral line hair cells using our previously defined damage scoring procedure.[13] YO-PRO-1 is a common vital dye used for staining viable lateral line hair cells in zebrafish.[18,19,21,32] The concentration of YO-PRO-1 (6 μM) and duration of exposure (20 min) were optimized for our purpose. After labeling, the larvae were rinsed thrice in embryo media and then anesthetized using 0.5 mM of MS-222 (tricaine methanesulfonate; Western Chemical, Inc.). The larvae were fixed in 2% paraformaldehyde for 1 h at room temperature and stored overnight in phosphate-buffered saline at 4°C. Fixed larvae were then mounted in 4%–6% methylcellulose (M7140; Sigma) in 0.2 mm silicone chambers and covered with No. 1.5 cover glass (64-0718; Warner Instruments) for confocal microscopy. Larvae were observed under a confocal microscope (Leica SP5) using 20× dry lenses. Treatment groups consisted of 3–7 fish each. Seven ventral neuromasts of the posterior lateral line (P3, P4, P5, P6, P7, P8, and P9) were selected for determination of the neuromast damage score per fish.[13] Each neuromast was assigned a damage score from 0 to 3. A score of 0 represents no damage with normal staining, 1 represents mild damage with moderate staining, 2 represents severe damage with poor staining, and 3 represents total hair cell or neuromast destruction with no staining. Seven scores per fish were then added to generate the total aggregate neuromast damage score. The lowest possible score for an individual fish is 0, representing no damage, with the highest possible score for a fish being 21, representing complete damage. Separate individuals (scorer A, B, and C) were trained in the counting technique and neuromast damage scores were generated independently with blinding of experimental conditions to insure unbiased assessment. The mean score of the three evaluators was used to determine the final neuromast damage score.

Swimming apparatus

Our newly developed swimming apparatus consists of multiple, professionally machined swimming tanks (Fig. 1A), each composed of 16 dedicated swimming lanes with removable swimming chambers for testing populations of zebrafish. A pump provides water flow from a common water reservoir through the 16 swimming lanes in each scalable tank through valves that regulate water flow rates precisely. Each fully functional swimming tank is very compact, measuring $\sim 100 \times 50 \times 40$ cm ($L \times W \times H$), and allows investigators to conduct 16 different behavioral experiments simultaneously. The system is completely scalable to accommodate a large array of such tanks, of which two have been built and are in use. The removable swimming chambers (Fig. 1B) are $12.5 \times 5 \times 5$ cm ($L \times W \times H$) in size and are covered on both ends by a nylon mesh that allows water flow through the chamber, while preventing the zebrafish from escaping from the swimming lane. We have confirmed that a mesh with 400 μm openings can hold the fish in the swimming chamber during the entirety of a behavioral experiment. These removable swimming chambers facilitate rapid transfer of zebrafish populations into and out of the swimming lanes, shortening the turnaround time between behavioral experiments.

Raspberry Pi microcomputer and NoIR infrared camera imaging system

A novel component of the newly developed system is an array of dedicated Raspberry Pi microcomputers (http://raspberrypi.org), each with a NoIR infrared camera (http://raspberrypi.org/products/pi-noir-camera) (Fig. 1C), manufactured by the Raspberry Pi Foundation (Cambridge, United Kingdom). This configuration captures high-definition (1080p) video for each swimming lane at 30 frames per second under infrared

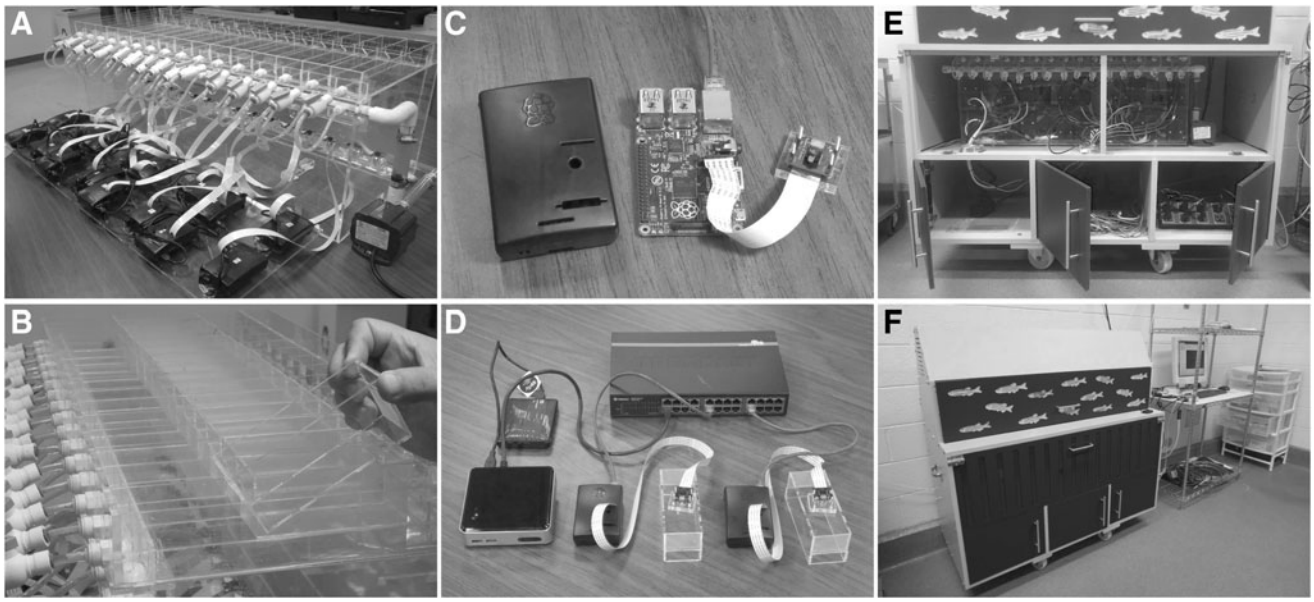

FIG. 1. **(A)** Swimming tank comprising a pump, flow control valves, water reservoir, and 16 individual swimming lanes. **(B)** Removable swimming chambers that can be inserted into each swimming lane to hold an experimental population of zebrafish. **(C)** Raspberry Pi microcomputer with the NoIR infrared camera. **(D)** Imaging system showing two Raspberry Pis with NoIR infrared cameras connected by a gigabit Ethernet switch to the control computer and the hard drive that stores data. **(E)** Cabinet housing the swimming tank and imaging system. **(F)** Complete behavioral assay system.

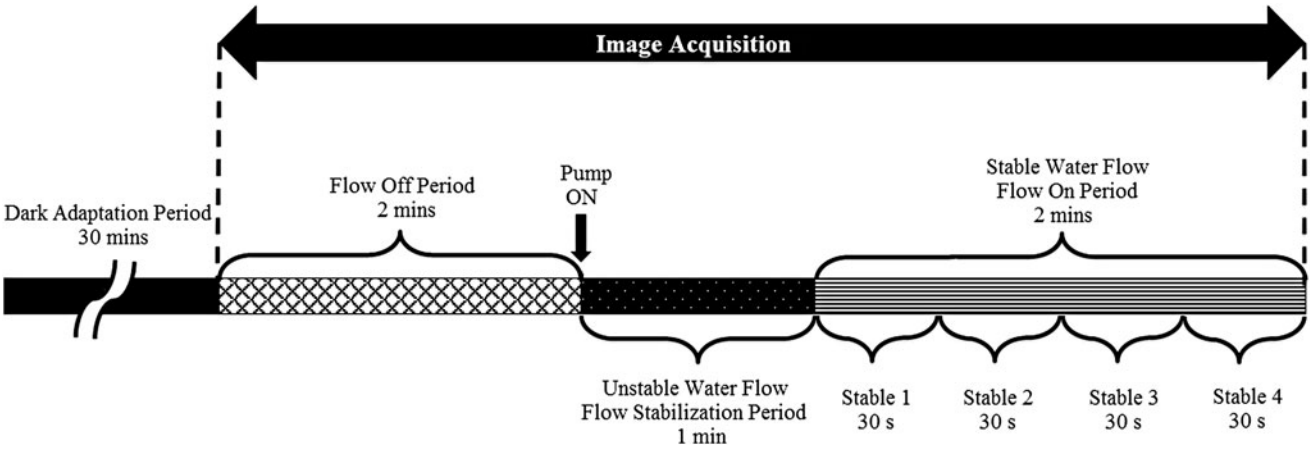

FIG. 2. Behavioral assay protocol showing the various periods: (1) dark adaptation (30 min), (2) flow off (2 min), (3) flow stabilization (1 min), and (4) flow on (2 min).

illumination. The Raspberry Pis are low-cost ($40 each) microcomputers that can be networked together through Ethernet. The NoIR infrared camera ($25 each) is a camera accessory for the Raspberry Pi, allowing picture and video capture under infrared lighting. The 16 Raspberry Pi microcomputers together with their respective infrared cameras form a low-cost, high-definition imaging system for each tank, which are accessed and controlled remotely by the control computer over a local high-speed intranet. Two Raspberry Pi microcomputers and their infrared cameras are shown (Fig. 1D) connected to a central control computer over the local intranet by a gigabit Ethernet switch. The swimming apparatus and Raspberry Pi imaging system are enclosed in a cabinet (Fig. 1E), and the entire behavioral assay system is seen in Figure 1F.

Behavioral assay protocol

Behavioral experiments using the swimming apparatus adhere to the following protocol (Fig. 2): a zebrafish population comprising 32 zebrafish larvae is placed in each lane through removable swimming chambers. These lanes are housed in darkness to remove visible light stimuli and are lit by overhead infrared lamps (IR-200-940; CM Vision, Houston, TX) for the purpose of imaging. The zebrafish are allowed to adapt to their dark surroundings (no visible light, just infrared) for 30 min, after which, infrared video data are acquired for 5 min, capturing their behavior. The 5 min of video data include three epochs: 2 min with no water flow, 1 min with water flow where the flow is allowed to stabilize, and 2 min with stable water flow to analyze the zebrafish response to an oncoming current.

Video analysis

To achieve high throughput, we automated the computation of RI by applying image processing algorithms that detect and segment every zebrafish in the acquired video (Fig. 3) and then compute their orientation with respect to the direction of oncoming current. Videos of swimming zebrafish were acquired from below each swimming lane, using infrared light sources placed overhead to capture zebrafish images in silhouette, examples of which can be viewed online (Supplementary Video S1, and Supplementary Video S2). Thus, zebrafish appear darker than the surrounding water. Several image analysis techniques[33,34] to detect bright

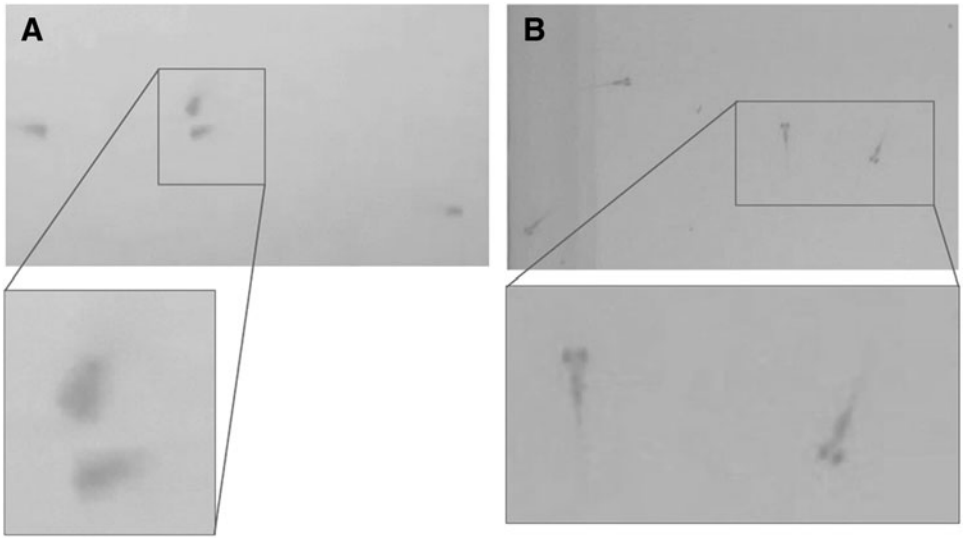

FIG. 3. **(A)** Image from six-lane system (480p). **(B)** New image from 16-lane system (1080p) showing higher resolution zebrafish swimming in the tank. Note that even the eyes of the zebrafish are discernible with the new system.

objects exist in the literature. Therefore, one approach is to invert the grayscale intensities of individual frames of the video as a preprocessing step, after which, an image processing algorithm called ''top hat transformation''[35] can be used to remove the background. Instead, we use the inverse of the top hat transformation, the ''bottom hat transformation,''[36] to detect dark objects, thereby eliminating the need for the preprocessing step. The bottom hat transformation effectively estimates the background in each frame, the subtraction of which from the original frame results in zebrafish foreground pixels being detected.

A disk-shaped structuring element with a radius of 41 pixels (twice the largest expected length of an individual zebrafish in our video data) is used in the bottom hat transformation. The structuring element is used to perform morphological closing (erosion of the dilated image) to estimate the background in each frame. The original frame is then subtracted from the estimated background to produce the bottom hat transformation of the frame. This process is followed by grayscale thresholding to retain pixels with grayscale intensity less than 20 to detect individual zebrafish in each frame. Finally, as a postprocessing step, detections with area less than 20 pixels are discarded to eliminate the detection of objects that are too small to be zebrafish. The parameters of the detection algorithm, namely structuring element size of radius 41 pixels, grayscale intensity threshold of 20, and size threshold of 20 pixels, were chosen in such a manner as to obtain a high number of accurate detections (high F-score[37]), while lowering the mean angular error and head/tail flip error percentage, after computing these error values for a large number of combinations of the three parameters.

Once the zebrafish are detected, principal components analysis[38] of the detected pixels of each zebrafish is used to determine its orientation with respect to the direction of the oncoming current. The principal component merely corresponds to the major *axis* of the zebrafish; so an inherent ambiguity exists as to which end of this axis corresponds to the head of the zebrafish. This ambiguity is resolved by bisecting the segmented zebrafish at the center of mass (mean column and row) by a line perpendicular to the major axis, and then computing which half has a greater number of detected pixels and defining this to be the direction of the head. The orientation is corrected for swimming chamber/camera tilt by determining the angle of orientation of the swimming chamber with respect to the horizontal. This angle of swimming chamber/camera tilt is typically small (<1°). The RI of the zebrafish test population is then determined as the percentage of zebrafish oriented within 30° of the direction of oncoming current (Fig. 4).

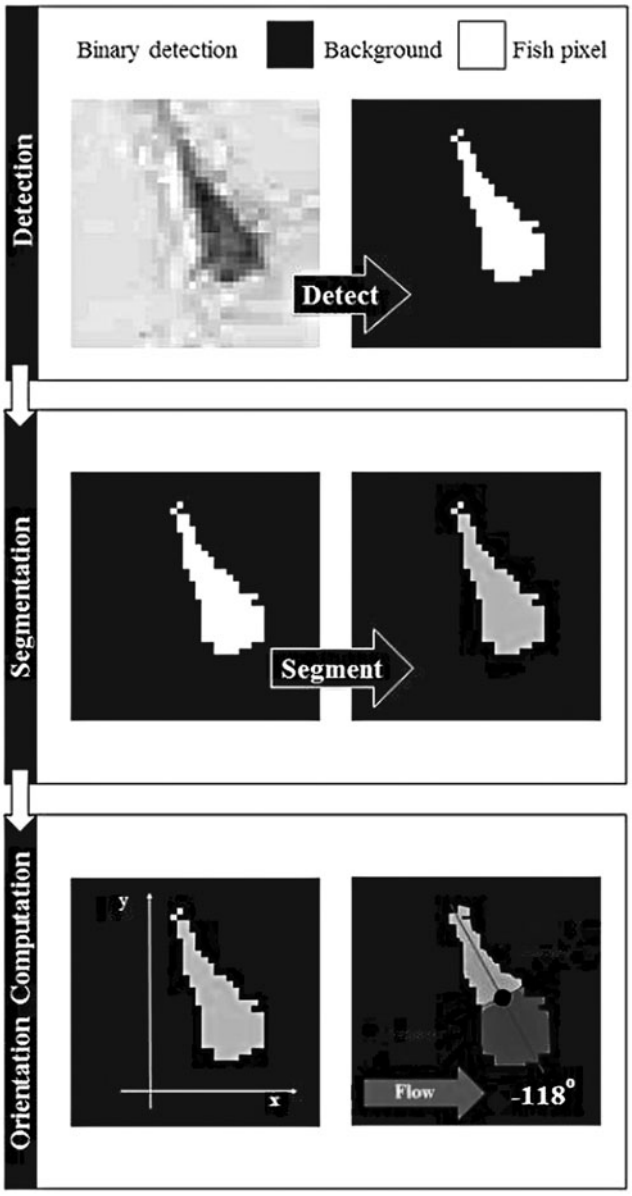

FIG. 4. Flowchart of the automated RI computation algorithm. Binary detection (differentiating between foreground and background) using the bottom hat transformation is performed to identify all the zebrafish in the frame. The segmentation step groups the detected pixels of each zebrafish into distinct objects. For each segmented zebrafish, its orientation with respect to the direction of oncoming current is determined using principal components analysis. RI, rheotaxis index.

Drug exposure experiments—cisplatin dose-dependent exposure

It is known that cisplatin causes hair cell and neuromast damage, including damage to hair cells and associated supporting cells in a dose-dependent manner.[21] To establish the sensitivity of our newly developed automatic behavioral assay for detecting damage caused by varying doses of cisplatin, we conducted dosing experiments similar to those performed in prior work.[13] Cisplatin solutions were prepared from powder (P4394; Sigma) in the embryo medium. Five dpf, zebrafish larvae were incubated in cisplatin at concentrations of 0, 250, 500, 750, and 1000 μM (Cis 0, Cis 250, Cis 500, Cis 750, and Cis 1000, respectively) for 4 h at 28.5°C ± 0.5°C, and then rinsed thrice with embryo media. RI for each group was then quantified automatically using our behavioral assay system.

Functional recovery experiments

Zebrafish lateral line hair cells can regenerate spontaneously after injury.[39,40] To test the functional validity of our new behavioral analysis system, we sought to determine

whether (1) anatomic recovery results in functional recovery of rheotaxis swimming behavior, and (2) our newly developed automated high-throughput behavior system can detect that functional recovery. The rationale for such experiments was that quantifying a potential gap between anatomic and functional recovery could serve as the foundation for assay development aimed at screening small molecules capable of stimulating tissue regeneration. Five dpf larvae were incubated in cisplatin at concentration of 1000 μM for 4 h at 28.5°C ± 0.5°C, rinsed thrice in embryo media, and raised in embryo media up to 72 h postinjury. Anatomic damage is quantified by our damage scoring procedure,[13] and RI for each treatment group is quantified using our behavioral assay system. Pearson's correlation coefficients of 0.94, 0.95, and 0.92 were observed in the damage scores generated by the three separate individuals, indicating consistency among scorers in manually assessing anatomic damage.

Aminoglycoside treatment

Aminoglycoside antibiotics are known as ototoxins,[19,20] with high risk of hearing loss in humans. To determine whether our behavioral assay could detect lateral line ototoxicity from ototoxins other than cisplatin, neomycin sulfate solutions (sc-3573A; Santa Cruz Biotechnology, Inc., Dallas, TX) were prepared from powder dissolved in the embryo medium. Five dpf zebrafish larvae were incubated in neomycin at concentrations of 0, 100, 200, 300, 400, and 500 μM (Neo 0, Neo 100, Neo 200, Neo 300, Neo 400, and Neo 500) for 60 min at 28.5°C ± 0.5°C, and then rinsed thrice with embryo media. The fish were then transferred to our behavioral assay system, and RI was quantified.

Results

Automated zebrafish detection

To validate our fully automated behavioral assay system, 49 frames of video data were analyzed manually by four human observers who were tasked with identifying the locations of each individual zebrafish in every frame and determining an estimate of the orientation of the zebrafish with respect to the direction of oncoming current. This manual process yielded ground truth data comprising 511–514 zebrafish and their corresponding orientation estimates.

Figure 5 shows the qualitative results of the detector with respect to one of the four human observers on a single frame of video. Dark gray circles represent true positives (TPs). For the purpose of error analysis, TPs are defined to be those detections that are within a Euclidean distance of 20 pixels (largest expected length of an individual zebrafish in our video data) from the ground truth location. The detections were constrained to a region of interest inside the innermost set of borders.

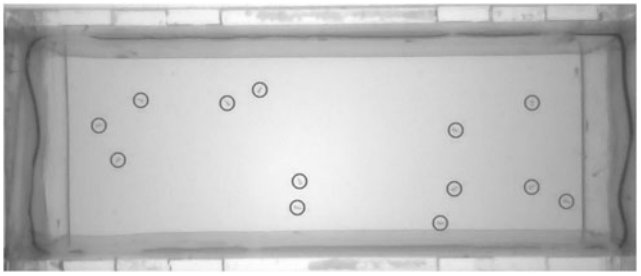

FIG. 5. Detection results versus observer 1. *Dark gray circles* represent true positives—zebrafish detected by our image analysis algorithm corresponding to manually identified zebrafish locations.

Table 1. Detection Accuracy

Auto vs.	*Truth*	*TP*	*FP*	*FN*	P	R	F
Observer 1	511	510	4	1	0.9922	0.9980	0.9951
Observer 2	511	508	7	3	0.9864	0.9941	0.9903
Observer 3	514	513	5	1	0.9903	0.9981	0.9942
Observer 4	511	506	6	5	0.9883	0.9902	0.9892

Precision (P) = TP/(TP + FP).
Recall (R) = TP/(TP + FN).
F-score (F) = $2PR/(P+R)$.
FN, false negatives; FP, false positives; TP, true positives.

Table 1 quantifies the results of the automatic zebrafish detection algorithm in terms of the following categories: (1) TPs, true zebrafish that were correctly detected; (2) false negatives (FNs), true zebrafish that were missed; and (3) false positives (FPs), detections not corresponding to a true zebrafish. Table 1 further quantifies detector performance in terms of precision, recall, and F-score.[37] Precision (P) is defined as the ratio of TPs to the number of detections (sum of TPs and FPs), TP/(TP + FP). Recall (R) is defined as the ratio of TPs to the number of true zebrafish (sum of TPs and FNs), TP/(TP + FN). F-score (F) quantifies the balance between precision and recall by computing their harmonic mean, $2PR/(P+R)$. Figure 6 shows a scatter plot of precision and recall for the automated detection algorithm against four human observers and the precision and recall between the human observers themselves.

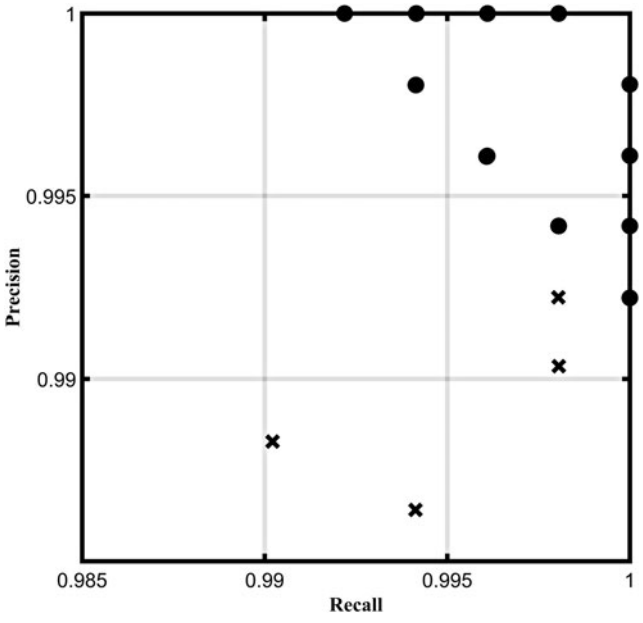

FIG. 6. Precision and recall values for the automated detector versus each human observer (×) and between each pair of human observers (•). Some precision and recall values between pairs of human observers are identical resulting in 11 distinct observations for 16 possible pairs.

Table 2. Orientation Computation Accuracy

Auto vs.	*Head/Tail error (%)*	*Mean error (degrees)*	*Std. Dev. (degrees)*
Observer 1	0.39	6.51	11.61
Observer 2	0.59	8.49	14.16
Observer 3	0.58	6.84	12.89
Observer 4	0.59	7.47	12.81

Head/Tail error: percentage error where the detection algorithm was unable to determine the orientation of the head of the zebrafish (distinguish it from the tail). Mean error: mean absolute difference between the direction of orientation of the ground truth and the detected zebrafish. Std. Dev.: standard deviation of the absolute difference between the direction of orientation of the ground truth and the detected zebrafish.

Automated computation of zebrafish orientation

The error of the automated orientation calculation was quantified relative to the manually estimated zebrafish orientations. For the TP detections, the head/tail flip error is computed as the percentage of fish whose automatically calculated orientation is determined to be opposite (absolute difference angle greater than 90°) of the manually estimated orientation. The angular error was computed as the absolute difference between the automatically calculated orientation and the manually estimated orientation. Table 2 shows the mean and standard deviation of the angular error, as well as the head/tail error. We also observed that 98% of detected zebrafish have angular error less than 30° as observed in the mean angular error distribution of the automated algorithm against four human observers (Fig. 7).

Automated RI computation

The RI computed automatically by our system was validated against the RIs computed from the four human observers. Figure 8 shows these RIs for each epoch: no water flow, unstable water flow, and stable water flow. An × indicates the RI computed by the automated image analysis algorithm, while a • indicates the RI computed by human observers. The automatically computed RIs at the various flow epochs were comparable to the RIs computed by four human observers, indicating that the automatic behavioral assay system produced results consistent with manual analysis. We noticed that the RI was around 20% during the no water flow epoch, which is close to the expected 16.67%, and the RI increased when the pump was turned on at the end of the no water flow epoch. The unstable water flow epoch showed a large variation in the data, as the water flow was turbulent. The stable water flow epoch was further subdivided into four time epochs, and the RI at each is also shown.

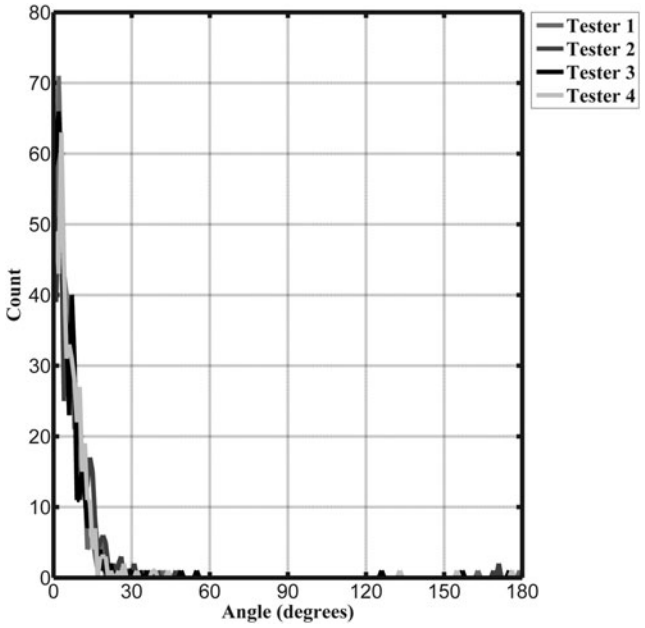

FIG. 7. Distribution of angular error with respect to four human observers.

Flow rate experiments

We conducted flow rate experiments to determine which flow rate produces optimum RI in our behavioral assay system. We varied the flow rate between 3 and 11 mm/s in multiple lanes and observed healthy populations of zebrafish that were expected to show a high ability to perform rheotaxis. Our swimming apparatus provided a uniform flow for set chambers and had no bias between lanes. At lower flow rates of 3.00–3.99 and 4.00–4.99 mm/s, the RIs at different flow epochs were random, which indicated that the flow rate was not high enough for the zebrafish to initiate rheotaxis. We observed flow rates of 5.00–5.99 and 8.00–8.99 mm/s exhibiting high RI (Figs. 9 and 10); however, at the highest flow rates, we noticed that some zebrafish were pushed toward the back end of the swimming chamber, whereupon they contacted mesh at the back of each swimming chamber and exhibited avoidance responses that artificially contributed to a higher RI. Based on these flow rate experiments, we determined that flow regulated at 5.00–5.99 mm/s yields optimal rheotactic behavior in our system.

Cisplatin dose-dependent exposure

We conducted dosing experiments with cisplatin similar to those performed in prior work[13] to validate that the automated high-throughput behavioral assay produced results consistent with our earlier proof-of-principle results (Fig. 11). Zebrafish test populations, comprising 32 five dpf larvae, were treated with varying dosages of cisplatin (0, 250, 500, 750, and 1000 μM) and their RIs were quantified by our behavioral assay system. The hypothesis of our prior work[13] states that higher dosages of cisplatin will result in higher zebrafish lateral line hair cell damage, which will manifest itself as a lowered ability to perform rheotactic behavior. In these studies, we observed that the RIs for control populations approached 80%, and there was a steady decrease in RI as the dose of the ototoxin increases. The error bars represent the standard deviation among the RI values of multiple test populations of zebrafish at the same dosage of cisplatin. These experiments validate that the high-throughput behavioral assay produces RIs that decrease with higher dosages of cisplatin, and is consistent with our prior publication.

Neomycin dose-dependent exposure

We studied similarities and differences in rheotaxis behavior for exposure to aminoglycoside (neomycin) versus platinum-based (cisplatin) ototoxins (Fig. 12). Interestingly,

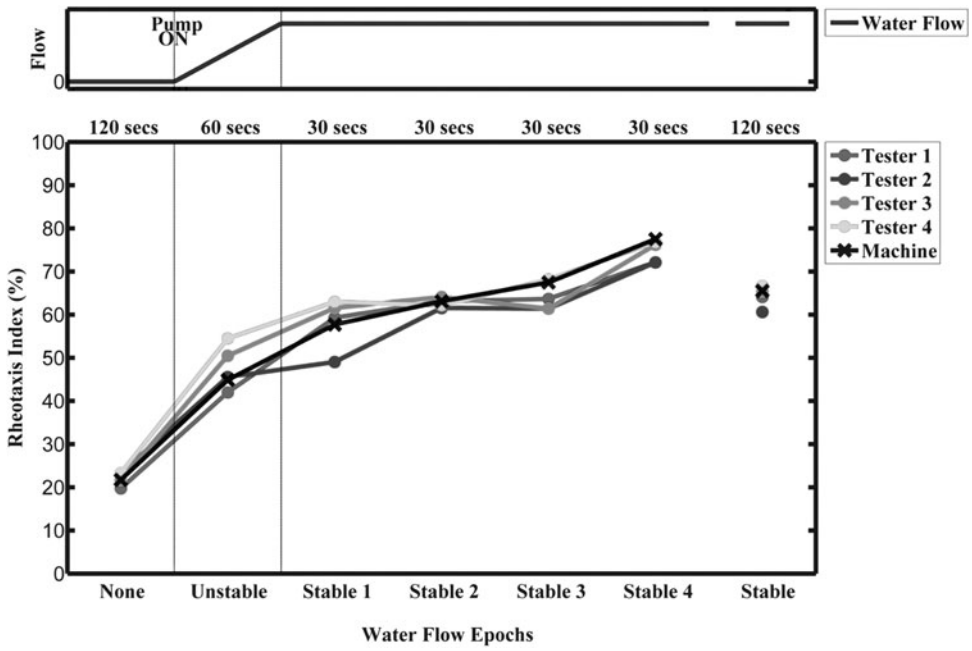

FIG. 8. RI computed by the machine (×) against human observers (•) for each of the three epochs. The automatically computed RI agrees with RIs computed by humans at each flow epoch.

the dose–response curves were quite different. The RI for Neo 100 was not statistically different than the control (Neo 0). The RIs for Neo 200, Neo 300, and Neo 400 were lower than control and very similar to each other, while Neo 500 produced the smallest mean RI. Statistical significance was assessed using a *t*-test, which produced statistically significant differences between control (Neo 0) and Neo 300 (p-value: 0.008) and between control (Neo 0) and Neo 500 (p-value: 0.002) after applying a Holm-Bonferroni correction.[41] The Holm-Bonferroni correction results in a failure to reject the null hypothesis for control (Neo 0) versus Neo 200 (p-value: 0.022) and between control (Neo 0) and Neo 400 (p-value: 0.022), while control (Neo 0) and Neo 100 produced a statistically insignificant p-value of 0.09. Because we were concerned about the overall toxicities of cisplatin and neomycin, we used 32 zebrafish larvae per test population with the expectation that perhaps 10% would die; however, we did not lose any fish during the experiments.

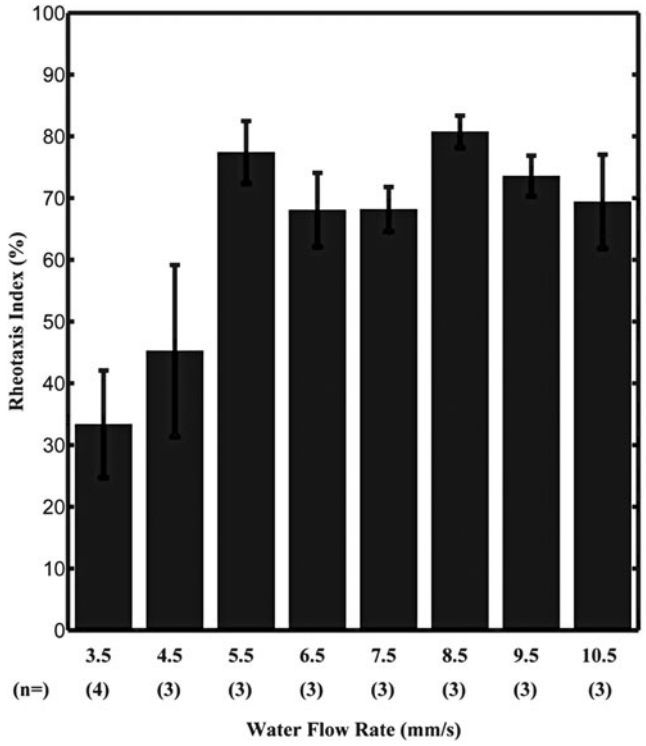

FIG. 9. RI as a function of water flow rate. The highest RIs were obtained for 5.00–5.99 and 8.00–8.99 mm/s.

Hair cell recovery experiments

Mackensie *et al.*[39] reported that cisplatin-induced damage does not recover completely in 72 h under anatomical observation. We observed similar anatomic assay results, wherein zebrafish lateral line cells recovered only partially from 1000 μM cisplatin exposure (mean damage score of 4.47) after 72 h, as opposed to a mean damage score of 15.73 immediately after treatment and 1.20 for control (no treatment). This partial recovery of cisplatin-induced anatomic damage is also observed in the partial recovery of behavioral function as demonstrated by our high-throughput behavioral assay (Fig. 13). The RIs for control, 0-h recovery, and 72-h recovery were 47.0%, 61.6%, and 76.3%, respectively, showing partial recovery at 72 h after treatment. Tests for statistical significance using a *t*-test produced p-values of 0.0034 between the 0-h recovery and control zebrafish treatment groups and 0.0120 between 72-h recovery and control groups for the behavioral assay, while the corresponding p-values for the anatomic assay were 5.817×10^{-9} and 0.0006, respectively, showing statistically significant differences at a significance level of 0.05 after applying a Holm-Bonferroni correction.[41] The fact that the behavioral function recovery closely follows the expected behavior based on the anatomic assay further validates that our fully automated high-throughput behavioral assay works as intended.

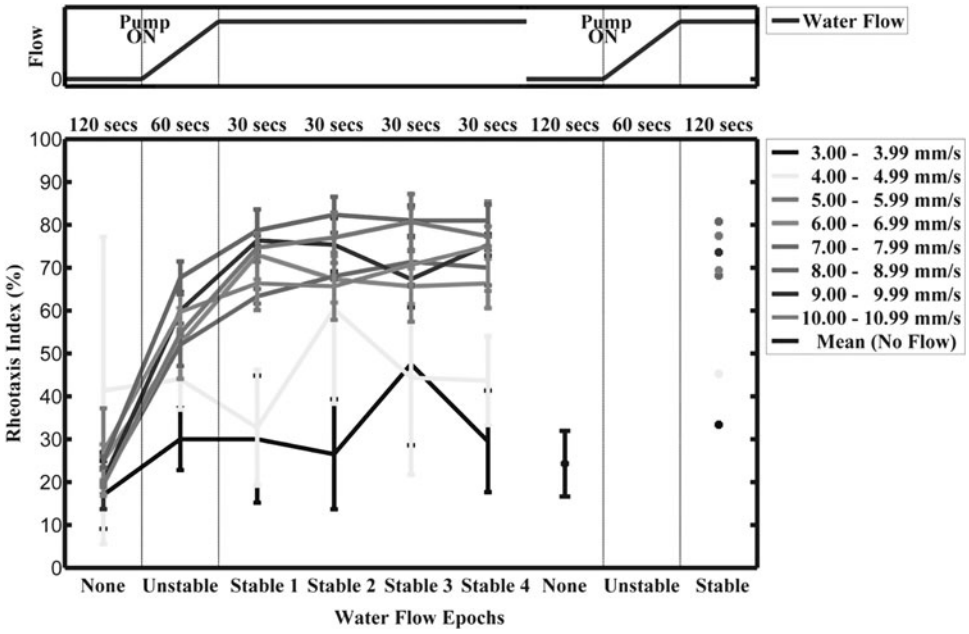

FIG. 10. RI for each water flow rate at each flow epoch. Flow rates of 3.00–3.99 and 4.00–4.99 mm/s show random RIs indicating that perhaps the water flow was not high enough for the zebrafish to initiate rheotaxis.

RI computation time

Previously, RI computation was done manually,[13] wherein the user had to visually observe still frames of video, manually identify all zebrafish in the frame, and painstakingly compute their orientation. This manual RI computation by trained experts consumed ~4 to 5 h per video of valuable time. Automated processing of videos on a 2007 quad-core Dell XPS 410 computer, with 1.6 GHz processor and 8 GB RAM, produces an average processing time of 5 min per video, whereas using high-performance computing clusters further reduces processing time to 1.33 min per video. The greatest contribution of our fully automated behavioral assay

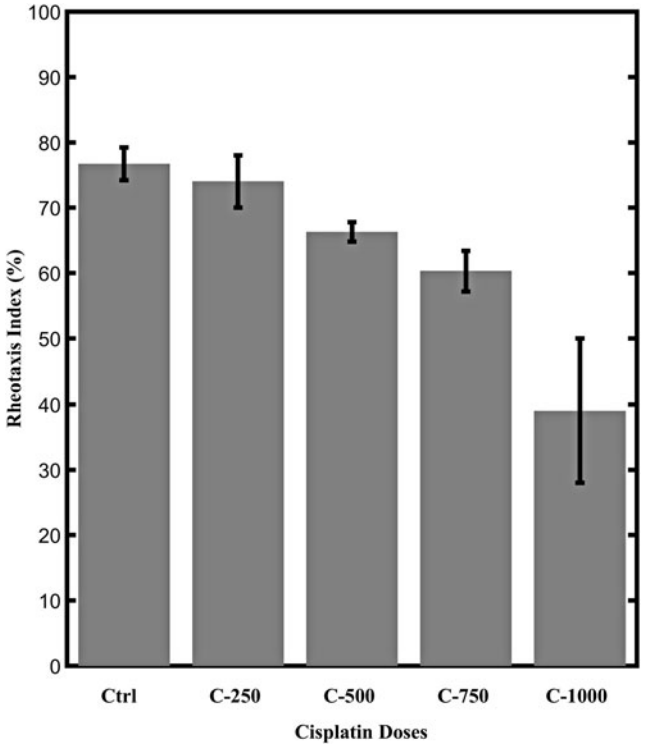

FIG. 11. RI for dosing experiments with cisplatin. The RIs automatically computed by our high-throughput behavioral assay are validated to be consistent with findings of prior work.

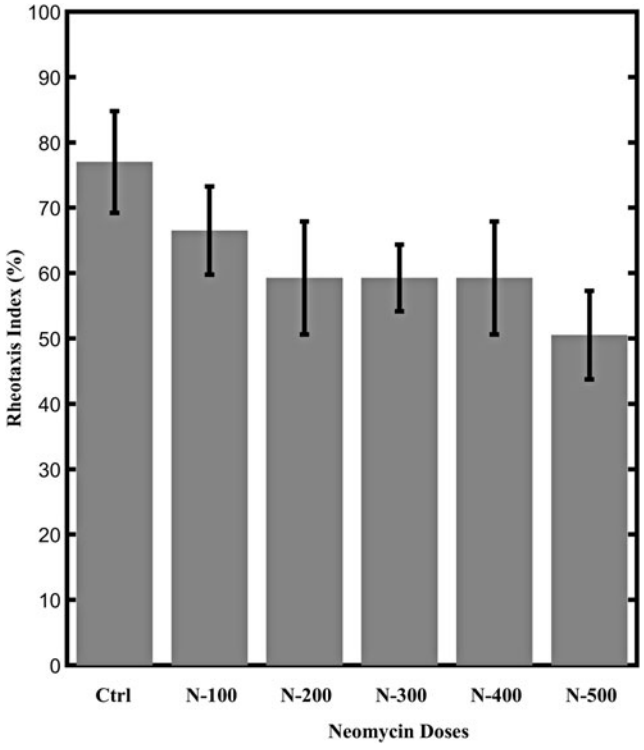

FIG. 12. RI for dosing experiments with neomycin sulfate.

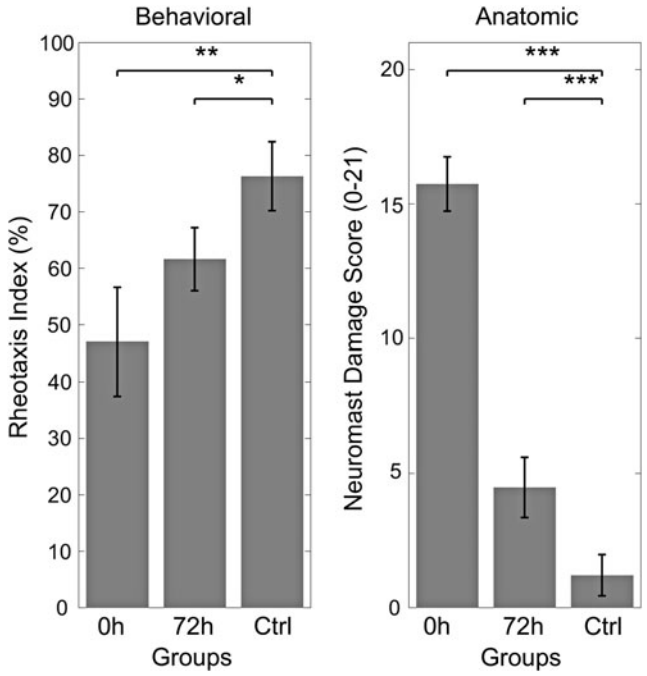

FIG. 13. Behavioral function and anatomic assay results of a cisplatin damage recovery experiment showing statistical significance between control, damaged (0-h recovery), and 72-h recovery groups. Significance levels: * 0.05, ** 0.01, and *** 0.001.

is in this enormous reduction of RI computation time, producing a truly high-throughput system that eliminates the tedium, and propensity for error associated with manual computation.

Discussion

There are no FDA-approved drugs, gene therapy programs, or stem cell treatments currently available for the prevention or treatment of hearing loss. Traditionally, chemopreventive agents have arisen from serendipitous explorations into small molecules, natural foods, herbs, or botanical resources, often being discovered from known homeopathic remedies,[42–44] while otoprotective compounds such as dexamethasone[45] have arisen out of empirical or experience-based discovery. In fact, phenotypic screens have identified novel drug targets and delivered more first-in-class medicines to human trials than traditional, more focused drug discovery efforts.[46] Still, while serendipity has been important in drug development, there is an immediate need to advance discovery platforms that operate at high-throughput levels with detailed and targeted molecular understanding.

Our group has developed and validated a next-generation, fully automated high-throughput behavioral assay that reliably uses zebrafish rheotaxis behavior as a surrogate biomarker for anatomic lateral line hair cell integrity. Using this system, a large number of behavioral experiments can be conducted in parallel, and rheotaxis values for each are computed in real-time after video acquisition. RI data tables are delivered to the investigator through intranet, thereby shortening analysis time from days (for manual analysis) to minutes. Our system is also highly scalable, as it can be expanded by sets of 16 lanes to any size necessary for studies of thousands of pharmaceutical compounds. This capacity facilitates testing multiple dosage and exposure time permutations per compound quickly and as needed. A review of zebrafish assays indicates that zebrafish swimming behavior has been widely used, for example, to study avoidance behavior and detect aquatic contamination,[47] nicotine-invoked locomotor response,[48] visual function,[49] and chemical toxicities to embryos.[50] While our group is not the first to study rheotaxis or use zebrafish behavioral assays incorporating rheotaxis measures to study ototoxicity, we believe this system to be highly suited for its primary purpose: high-throughput drug discovery targeting hearing loss.

Experiments comparing automated image analysis to manual analysis by trained experts have confirmed high precision and recall for our detection algorithm. Zebrafish larvae are reliably detected while keeping FPs to a minimum. Combined with an accurate orientation computation algorithm having a mean error ranging from 6.5° to 8.5°, our automated system ensures a highly accurate RI for the zebrafish population under test, as evidenced by the RI epoch plots that also fall within inter-operator performance. In fact, dose–response experiments validate that the behavioral assay captures the linear relationship between zebrafish anatomical hair cell damage and rheotactic behavior. In addition, recovery experiments show that the behavioral assay closely achieves the same statistically significant results, as produced by the anatomic assay on various treatment groups, therefore establishing that our system can detect functional recovery in the presence of anatomic damage. Using this assay to test a standardized ototoxic dose of cisplatin (or other toxins) against varying doses of compounds that potentially protect or regenerate hair cells may facilitate rapid translation of candidate drugs (currently no FDA-approved treatment exists) into preclinical mammalian models of hearing loss.

Platinum-based chemotherapeutic drugs and aminoglycosides are two major classes of drugs that cause hearing loss in patients through reactive oxygen species (ROS)-mediated hair cell death.[17,51–53] In this study, we used both cisplatin and neomycin to assess the capabilities of our high-throughput behavioral assay system to detect rheotaxis damage induced by different ototoxins and mediated by lateral line hair cells.

Coffin *et al.*[54] and Harris *et al.*[16] observed significant hair cell death (anatomic assay) at 100 μM of neomycin concentration, and the degree of damage did not change in higher concentrations. This result parallels our findings for behavioral assay results using neomycin. We noted a statistically significant change in RI at Neo 200 μM, which then remains the same at higher concentrations, with only a slight reduction in mean RI at 500 μM. Using our behavioral assay system, we were able to confirm the findings of prior work.[16,54] This result further validates that our fully automated high-throughput behavioral assay system is reliable as a surrogate biomarker for anatomic hair cell damage, not only for cisplatin but also for aminoglycosides like neomycin.

Cisplatin exposure at 1000 μM reduces RI to $\sim$40% (Fig. 11), while neomycin exposure at 500 μM reduces RI to $\sim$50% (Fig. 12). Anatomically, both Cis 1000 and Neo 500 cause comparably severe damage to hair cells,[13,16,54] while behaviorally, there is a 10% difference between the RIs. Cisplatin is a chemotherapeutic agent that can treat various types of solid tumors, although it has dosage limitations due to ototoxicity, neurotoxicity, bone marrow suppression, nephrotoxicity, and so on, in humans.[17] Higher concentrations of cisplatin

may affect other zebrafish systems—neurotransmitters, motor neurons, and so on, which may affect rheotaxis swimming behavior. This could be one of the reasons why the RI of cisplatin 1000 μM is lower than the RI of neomycin 500 μM. In addition, hair cell death mechanisms caused by cisplatin and neomycin are different, and several studies show that susceptibility to neomycin increases in later development stages of zebrafish.[55] Those factors could also affect rheotaxis swimming behavior in zebrafish, and we have to understand this to research otoprotective reagents.

Automated behavioral assays overcome inherent limitations of relying solely on anatomic assays of zebrafish lateral line hair cell integrity, namely (1) the comprehensive assessment-wide drug dose parameters, (2) permutations for varying durations of drug exposure at each dose, (3) permutations for varying the timing for said exposure (pretreatment, simultaneous exposure, posttreatment, and so on), and (4) determining whether anatomically preserved hair cells are truly functional. By limiting the anatomic assay to only a fraction of our most promising drugs that pass through the fully automated high-throughput behavioral assay, labor and costs are minimized, while throughput is dramatically enhanced. Finally, ongoing efforts toward improving the development of zebrafish hair cell culture systems, refining immunostaining techniques both for fixed and *in situ* preparations, reliably staining mitochondrial tissues within lateral line hair cells, and quantifying measures of ROS generation, both in water and within neuromasts, may allow us to work (backwards) toward analyzing the mechanisms of action for our most promising drug candidates.

Our fully automated high-throughput behavioral assay system produces results consistent with prior work in ototoxin-induced lateral line hair cell damage that manifests itself as a lowered functional ability to perform rheotaxis.

Acknowledgments

This project was funded by the BIO5 Institute at The University of Arizona, the Department of Otolaryngology at The University of Arizona, and Cochlear Americas, Inc. The latter did not influence the content of this manuscript. The authors would like to express gratitude to the University Animal Care at The University of Arizona for their excellent care of our zebrafish.

Disclosure Statement

No competing financial interests exist.

References

1. Korver AM, Konings S, Dekker FW, Beers M, Wever CC, Frijns JH, *et al.* Newborn hearing screening vs. later hearing screening and developmental outcomes in children with permanent childhood hearing impairment. JAMA 2010;304:1701–1708.
2. Cruickshanks KJ, Wiley TL, Tweed TS, Klein BE, Klein R, Mares-Perlman JA, *et al.* Prevalence of hearing loss in older adults in Beaver Dam, Wisconsin. The Epidemiology of Hearing Loss Study. Am J Epidemiol 1998;148:879–886.
3. Gates GA, Cooper JC, Jr., Kannel WB, Miller NJ. Hearing in the elderly: the Framingham cohort, 1983–1985. Part I. Basic audiometric test results. Ear Hear 1990;11:247–256.
4. Moscicki EK, Elkins EF, Baum HM, McNamara PM. Hearing loss in the elderly: an epidemiologic study of the Framingham Heart Study Cohort. Ear Hear 1985;6:184–190.
5. Martini A, Castiglione A, Bovo R, Vallesi A, Gabelli C. Aging, cognitive load, dementia and hearing loss. Audiol Neurotol 2014;19 (Suppl. 1):2–5.
6. Lin FR. Hearing loss in older adults: who's listening? JAMA 2012;307:1147–1148.
7. Berg AL, Spitzer JB, Garvin JH, Jr. Ototoxic impact of cisplatin in pediatric oncology patients. Laryngoscope 1999;109:1806–1814.
8. Laurell G, Jungnelius U. High-dose cisplatin treatment: hearing loss and plasma concentrations. Laryngoscope 1990;100:724–734.
9. Rybak LP, Whitworth CA, Mukherjea D, Ramkumar V. Mechanisms of cisplatin-induced ototoxicity and prevention. Hear Res 2007;226:157–167.
10. Henderson D, Bielefeld EC, Harris KC, Hu BH. The role of oxidative stress in noise-induced hearing loss. Ear Hear 2006;27:1–19.
11. Rybak LP, Ramkumar V. Ototoxicity. Kidney Int 2007;72: 931–935.
12. Hoshino T, Tabuchi K, Nishimura B, Tanaka S, Nakayama M, Ishii T, *et al.* Protective role of Nrf2 in age-related hearing loss and gentamicin ototoxicity. Biochem Biophys Res Commun 2011;415:94–98.
13. Niihori M, Platto T, Igarashi S, Hurbon A, Dunn AM, Tran P, *et al.* Zebrafish swimming behavior as a biomarker for ototoxicity-induced hair cell damage: a high-throughput drug development platform targeting hearing loss. Transl Res 2015;155:440–450.
14. Thomas AJ, Wu P, Raible DW, Rubel EW, Simon JA, Ou HC. Identification of small molecule inhibitors of cisplatin-induced hair cell death: results of a 10,000 compound screen in the zebrafish lateral line. Otol Neurotol 2015;36: 519–525.
15. Ton C, Parng C. The use of zebrafish for assessing ototoxic and otoprotective agents. Hear Res 2008;208:79–88.
16. Harris JA, Cheng AG, Cunningham LL, MacDonald G, Raible DW, Ruble EW. Neomycin-induced hair cell death and rapid regeneration in the lateral line of zebrafish (*Danio rerio*). J Assoc Res Otolaryngol 2003;04:219–234.
17. Owens KN, Coffin AB, Hong LS, Bennett KO, Rubel EW, Raible DW. Response of mechanosensory hair cells of the zebrafish lateral line to aminogylcosides reveals distinct cell death pathways. Hear Res 2009;253:32–41.
18. Coffin AB, Ou H, Owens KN, Santos F, Simon JA, Rubel EW, *et al.* Chemical screening for hair cell loss and protection in the zebrafish lateral line. Zebrafish 2010;7:3–11.
19. Ou HC, Santos F, Raible DW, Simon JA, Rubel EW. Drug screening for hearing loss: Using the zebrafish lateral line to screen for drugs that prevents and cause hearing loss. Drug Discovery Today 2010;15:265–271.
20. Buck LM, Winter MJ, Redfern WS, Whitfield TT. Ototoxin-induced cellular damage in neuromasts disrupts lateral line function in larval zebrafish. Hear Res 2012;284:67–81.
21. Ou HC, Raible DW, Rubel EW. Cisplatin-induced hair cell loss in zebrafish (*Danio rerio*) lateral line. Hear Res 2007; 233:46–53.
22. Arnold GP. Rheotropism in fishes. Biol Rev Camb Philos Soc 1974;49:515–576.
23. Suli A, Watson GM, Rubel EW, Raible DW. Rheotaxis in larval zebrafish is mediated by lateral line mechanosensory hair cells. PLoS One 2012;7:e29727.

24. Nemeth MJ, Krueger CC, Josephson DC. Rheotactic response of two strains of juvenile landlocked atlantic salmon: implications for population restoration. Trans Am Fish Soc 2003;132:904–912.
25. Van Trump WJ, McHenry MJ. The lateral line system is not necessary for rheotaxis in the Mexican blind cavefish (*Astyanax fasciatus*). Integr Comp Biol 2013;53:799–809.
26. Kulpa M, Bak-Coleman J, Coombs S. The lateral line is necessary for blind cavefish in non-uniform flow. J Exp Biol 2015;218:1603–1612.
27. Montgomery JC, Baker CF, Carton AG. The lateral line can mediate rheotaxis in fish. Nature 1997;389:960–963.
28. Arnold GP, Weihs D. The hydrodynamics of rheotaxis in the plaice (Pleuronectes Platessa L.). J Exp Biol 1977;75: 147–169.
29. McNeil PL, Boyle D, Henry TB, Handy RD, Sloman KA. Effects of metal nanoparticles on the lateral line system and behaviour in early life stages of zebrafish (*Danio rerio*). Aquat Toxicol 2014;152:318–323.
30. Olszewski J, Haehnel M, Taguchi M, Liao JC. Zebrafish larvae exhibit rheotaxis and can escape a continuous suction source using their lateral line. PLoS One 2012;7: e36661.
31. Olive R, Wolf S, Dubreuil A, Bormuth V, Debregeas G, Candelier R. Rheotaxis of larval zebrafish: behavioral study of a multi-sensory process. Front Syst Neurosci 2016; 10:14.
32. Santos F, MacDonald G, Rubel EW, Raible DW. Lateral line hair cell maturation is a determinant of aminoglycoside susceptibility in zebrafish (*Danio rerio*). Hear Res 2006; 213:25–33.
33. Ruusuvuori P, Aijo T, Chowdhury S, Garmendia-Torres C, Selinummi J, Birbaumer M, *et al.* Evaluation of methods for detection of fluorescence labeled subcellular objects in microscope images. BMC Bioinformatics 2010;11:1–17.
34. Smal I, Loog M, Niessen W, Meijering E. Quantitative comparison of spot detection methods in fluorescence microscopy. IEEE Trans Med Imaging 2010;29:282–301.
35. Kimori Y, Baba N, Morone N. Extended morphological processing: a practical method for automatic spot detection of biological markers from microscopic images. BMC Bioinformatics 2010;11:1–13.
36. Serra J: Image Analysis and Mathematical Morphology. Academic Press, Inc., Orlando, FL, 1983.
37. Fawcett T. An introduction to ROC analysis. Pattern Recognit Lett 2006;27:861–874.
38. Duda RO, Hart PE, Stork DG: Pattern Classification, 2nd ed. Wiley-Interscience, New York, NY, 2000.
39. Mackenzie SM, Raible DW. Proliferative regeneration of zebrafish lateral line hair cells after different ototoxic insults. PLoS One 2012;7:e47257.
40. Lush ME, Piotrowski T. Sensory hair cell regeneration in the zebrafish lateral line. Dev Dyn 2014;243:1187–1202.
41. Holm S. A simple sequentially rejective multiple test procedure. Scand J Statist 1979;6:65–70.
42. Patterson SL, Colbert Maresso K, Hawk E. Cancer chemoprevention: successes and failures. Clin Chem 2013;59: 94–101.
43. Gerhauser C. Cancer chemoprevention and nutriepigenetics: state of the art and future challenges. Top Curr Chem 2103; 329:73–132.
44. Madhunapantula SV, Robertson GP. Chemoprevention of melanoma. Adv Pharmacol 2012;65:361–398.
45. Chirtes F, Albu S. Prevention and restoration of hearing loss associated with the use of cisplatin. BioMed Res Intl 2014;2014:925485.
46. Swinney DC. Phenotypic vs. target-based drug discovery for first-in-class medicines. Clin Pharmacol Ther 2013;93: 299–301.
47. Nuber LK, Skulovich O, Hartmann S, Seiler TB, Cofalia C, Schuettrumpf H, *et al.* A sensitive biomarker for the detection of aquatic contamination based on behavioral assays using zebrafish larvae. Ecotoxicol Environ Saf 2016;133: 271–280.
48. Mora-Zamorano FX, Svoboda KR, Carvan MJ III. The nicotine-evoked locomotor response: a behavioral paradigm for toxicity screening in zebrafish (*Danio rerio*) embryos and eleutheroembryos exposed to methylmercury. PLoS One 2016;11:e0154570.
49. Scott CA, Marsden AN, Slusarski DC. Automated, high-throughput, in vivo analysis of visual function using the zebrafish. Dev Dyn 2016;245:605–613.
50. Olivares CI, Field JA, Simonich M, Tanguay RL, Sierra-Alvarez R. Arsenic (III, V), indium (III), and gallium (III) toxicity to zebrafish embryos using a high-throughput multi-endpoint in vivo developmental and behavioral assay. Chemosphere 2016;148:361–368.
51. Schacht J, Talaska AE, Rybak LP. Cisplatin and aminoglycoside antibiotics: hearing loss and its prevention. Anat Rec 2012;285:1837–1850.
52. Huth ME, Ricci AJ, Cheng AG. Mechanisms of aminoglycoside ototoxicity and targets of hair cell protection. Int J Otolaryngol 2011;2011:938861.
53. Rybak LP, Mukherjea D, Jajoo S, Ramkumar V. Cisplatin induced ototoxicity and protection: clinical and experimental studies. Tohoku J Exp Med 2009;219:177–186.
54. Coffin AB, Williamson KL, Mamiya A, Raible DW, Rubel EW. Profiling drug-induced cell death pathways in the zebrafish lateral line. Apoptosis 2013;18:393–408.
55. Monroe JD, Rajadinakaran G, Smith ME. Sensory hair cell death and regeneration in fishes. Front Cell Neurosci 2015;9:131.

Address correspondence to:
Abraham Jacob, MD
Ear & Hearing
Center for Neurosciences
2450 East River Road
Tucson, AZ 85718

E-mail: ajacob@neurotucson.com